Permeability and Diffusion of Gases in Segmented Polyurethanes: Structure–Properties Relations

G. GALLAND and T. M. LAM*

Laboratoire des Matériaux Macromoléculaires, URA CNRS n° 507, Institut National des Sciences Appliquées de Lyon, 20, Avenue A. Einstein, 69621 Villeurbanne Cedex, France

SYNOPSIS

To determine the structure–transport properties relations, we synthetized segmented polyether polyurethane with increasing rigidity. The formulation is based on poly(tetramethylene oxide diol) (PTMO) of different molecular weights, diphenylmethane diisocyanate (MDI), and butanediol (BD). The synthesis is effectuated in bulk. The phase-separation degree of the soft segments is determined by ΔC_p measurements. The volume fractions and compositions of soft and hard phases are calculated with the help of T_g values. The polyurethanes studied correspond to three types of morphology: soft-phase matrix, phase-inversion, and hard-phase matrix. The best phase segregation is observed in the phase-inversion region. The time-lag method is used for determining the permeability, diffusion, and solubility coefficients of gases (He, O_2, N_2, CO_2, Freon 11) in polyurethane at different temperatures. Activation energies of permeation and diffusion and dissolution energy are calculated. The most important factor in diffusion is the chain mobility in the soft phase, which is represented with a good approximation by $\overline{M_n}$, the molecular weight of soft segments. The phase-inversion region where the ratio surface/volume is minimum gave the lowest solubility coefficient. Freon 11 presents a particular interaction with polyurethane; polyurethane membranes are broken when immerged in Freon 11, except the one which has the morphology of the inversion region. © 1993 John Wiley & Sons, Inc.

INTRODUCTION

Properties of segmented polyurethanes are greatly influenced by the microphase-separation degree. Numerous studies have treated with problem, using different techniques (see, e.g., Ref. 1). A few articles have concerned the relation between structure and transport properties.[2–5] Mac Bride et al.[2] measured diffusion coefficients and activation energies for a series of block polyurethanes that are well characterized. These authors used the flow technique with a quadrupole mass spectrometer as a detecting device. The permeability coefficients are not determined. Ziegel[3] used a similar technique and determined the permeability and diffusion coefficients of simple gas (He, H_2, Ar, N_2, O_2) through industrial polyether and polyester polyurethanes. Nevertheless, chemical formulations are not given. For Ar, O_2, and N_2, Ziegel gave two values of diffusion constants, corresponding, respectively, to soft and hard blocks. Mac Bride et al., using a similar technique, did not observe two different values for the diffusion coefficient.

Knight and Lyman[4] studied the influence of the chemical structure of polyurethanes and polyurethanes–ureas on the permeability of single gases (the diffusion coefficients are not measured). Correlations have been established with the molecular mass of diol oligomers, the chemical nature of these oligomers [poly(oxypropylene glycol) (POP) or poly(oxyethylene glycol) (POE)], and the chemical nature of the chain extender.

Andrady and Sefcik[5] prepared "model" networks of polyurethane by reacting poly(propylene glycol)

* To whom correspondence should be addressed at Laboratoire de Génie et Matériaux Textiles, Ecole Nationale Supérieure des Arts et Industries Textiles, 59070 Roubaix Cédex 01, France.

Journal of Applied Polymer Science, Vol. 50, 1041–1058 (1993)
 CCC 0021-8995/93/061041-18

with a triisocyanate cross-linking agent and measured the permeability of H_2 and CO between the membranes formed from these networks. This work demonstrates an exponential relationship between the logarithm of the permeability coefficient and the inverse of molecular weight between cross-links, $\overline{M_c}$, $\overline{M_c}$ being assumed to be equal to the molecular weight $\overline{M_n}$ of the starting prepolymer. As the gas solubility coefficients toward the chain length show little dependence on cross-link density, the observed dependence of the permeability coefficients should reflect the dependence of the diffusion coefficients.

This article deals with the synthesis and the characterization of some segmented polyurethanes, gives the results of the determination of the permeability, diffusion, and solubility coefficients, and discusses the results. We proceeded by starting with a soft material and increasing its rigidity by variation of the molecular weight of the polyols. Therefore, we synthesized polyether polyurethanes based on poly(tetramethyleneoxide diol) (PTMO), diphenylmethane diisocyanate (MDI), and 1,4-butanediol (BD).

EXPERIMENTAL

Synthesis

The number-average molecular weight, $\overline{M_n}$, of the PTMO oligomer was determined by cryometry and the functionality by ^{1}H-nuclear magnetic resonance.[6] The characteristics of the oligomers are given in the Table I. MDI (Dow) and BD (Fluka) were used without purification.

The polyurethanes were prepared in two steps: The first one was the reaction in bulk between the PTMO oligomer and MDI at 80°C, with strong stirring for 2 h under vacuum. The second step was the addition of BD. After the introduction, stirring was continued for 1 min and the mixture was cured in a mold for 24 h at 80°C. The polyurethane was designated by the $\overline{M_n}$ value of PTMO, followed by the numbers of moles of PTMO–MDI–BD, which indicated the used formulation.

DSC Measurements

A Mettler TA3000 microcalorimeter was used with heating rates of 5 or 7.5°C/min. The temperature values were obtained with a precision of +0.5°C, and the enthalpy values, with a probable error of about ±2%. For the amorphous soft phase, a cooling rate of 10°C/min was used from room temperature to −170°C with a sample weight of about 15 mg. For crystalline soft segments, cells were quenched at 40°C by putting them into liquid nitrogen to obtain fully amorphous soft segments for ΔC_p measurements. When pure PTMO is quenched, the sample weight must be inferior to 5 mg to eliminate crystallinity. The fully amorphous character of the structure was verified by measuring the recrystallization enthalpy. Scanning from −170°C provides excellent base lines for ΔC_p determination. Five to 10 runs were made for each product. The difference of ΔC_p between two different runs was not more ±5%. Therefore, the average ΔC_p can be estimated within ±2%. The values of the ΔC_p measurements are given in Table II.

Mechanical Measurements

Mechanical measurements were made on a traction machine J. J. Lloyd 5002, with a normalized H_3 size sample: total length = 50 mm; length and width of the narrow part = 17 and 4 mm; thickness = 1 mm. The traction speed was 15 mm/min.

Permeability Measurements

The membranes were obtained by hot pressing; their thicknesses were about 200 μm. The time-lag method was used for determining diffusion and permeability coefficients. The scheme of the apparatus is shown in Figure 1. Before diffusion experiments, the membrane was degassed during 24 h under a secondary

Table I Characteristics of Starting Oligomers

POTM Oligomer	$\overline{M_n}$ ± 5%	$\overline{F_n}$ ± 5%	T_g (°C) ± 0.5%
TERACOL 2000 DuPont	2400	1.8	−92.8
	2030	1.7	−93.2
POLYTHF 1000 BASF	1410	2.8	−97.4
POLYTHF 650 BASF	890	2.7	−99.6

Table II Characteristics of Soft Phase, Determined by DSC

Polyurethane	% in Weight of Soft Segment	% in Weight of Hard Segment	Glass Transition Temperature of Soft Phase T_g ± 0.5°C	Melting Point of Soft Phase (°C)	ΔC_{p_2} (±2%) (J/g °C)	$\Delta C_{p_2}/\Delta C^1_{p_2}$ (%)
PUR 2400 1/3/2	74.2	25.8	−75	16.4	0.534	63.6
PUR 2030 1/3/2	74.2	27.8	−76.2	14.2	0.512	61
PUR 2030 1/7/6	51.9	48.1	−80.8	10.0	0.533	63.4
PUR 1410 1/3/2	51.8	48.2	−70.3	—	0.618	73.6
PUR 890 1/3/2	41.7	58.3	−52.8	—	0.464	55.2
PUR 890 1/2/1	51.7	48.3	−47.8	—	No phase separation	

vacuum at 60°C. The membrane temperature was regulated at ±0.1°C. The temperatures varied from room temperature to 75°C. The gases used were the purest ones supplied by Air Liquide: He N55, N_2 N48, O_2 N48, and CO_2 N45. The Freon used was trichlorofluoromethane, CCl_3F, obtained under the designation of Forane F11 and was used without purification.

The diffusion coefficient, D, and permeability coefficient, P, are, respectively, given by

$$D = l^2/6\theta \text{ cm}^2/\text{s} \quad (1)$$

$$P = 273\,V \cdot p \cdot l/A \cdot T \cdot p \text{ cm}^3 \text{ (NTP)}$$
$$\text{cm/cm}^2 \text{ s atm} \quad (2)$$

where l is the membrane thickness (about 200 μm); θ, the time-lag (s); V, the volume (cm^3) occupied by the gas during the diffusion experiment; p, the increased rate of gas pressure in V during the experiment, in steady state ($mmHg\ s^{-1}$); A, the mem-

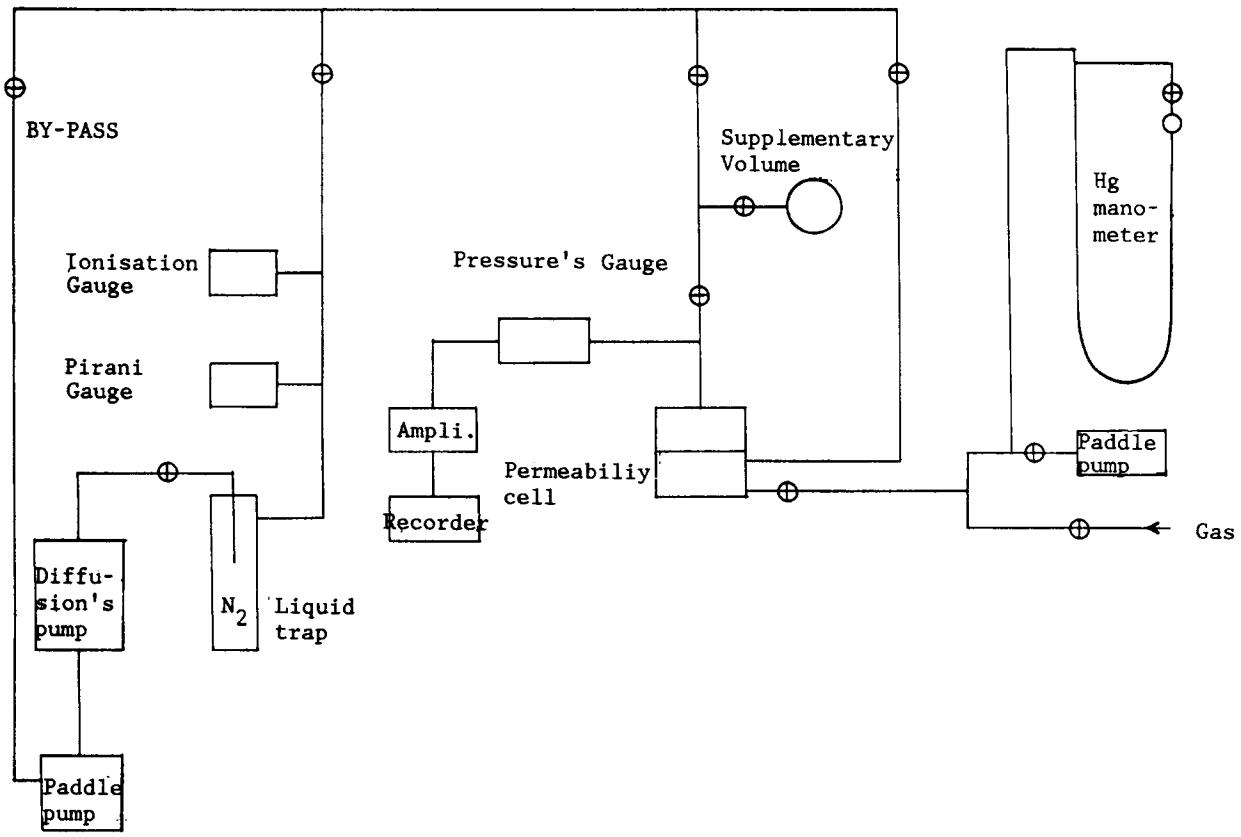

Figure 1 Scheme of permeability apparatus.

brane area; T, the temperature of the permeability cell; and p, the gas pressure of the membrane (about atmospheric pressure). The solubility coefficient, S, is calculated by

$$S = P/D \text{ cm}^3 \text{ (NTP) cm}^{-3} \text{ atm}^{-1} \quad (3)$$

RESULTS AND DISCUSSION

DSC Characterization

In the characterization of the morphology of polyurethane (PU), we wanted to determine the proportion of the soft and hard phases. A quantitative evaluation of the degree of phase separation is possible by DSC experiments.[7,8] This method consists of measuring the heat-capacity change $\Delta C_{p(s)}$ at the glass transition of the soft phase and comparing the value with $\Delta C^0_{p(s)}$, a value corresponding to a total microphase separation. $\Delta C^0_{p(s)}$ is considered as equal to that of the pure PTMO oligomer (84 J/g K). Therefore, we considered as negligible the variation of ΔC_p introduced by the mobility restriction of the soft segments due to the physical reticulation by hard nodules. The $\Delta C_{p(s)}/\Delta C^0_{p(s)}$ ratio listed in Table II measures the degree of microphase separation, giving the quantity of soft segments in the soft phase. This quantity is preponderant in the soft phase and we could assimilate this volume fraction as the one of the whole soft phase. However, a rough determination of the contribution of hard segments in the soft phase is possible and will be made below.

An estimation of the amount of soft and hard segments in the soft phase can be obtained by the Fox equation:

$$\frac{1}{T_g} = \frac{W_S}{T_{gS}} + \frac{W_H}{T_{gH}} \quad (4)$$

W_S is the mass fraction of soft segments in the soft phase; W_H (= 1 − W_S), the mass fraction of hard segments; T_g, the glass transition of the soft phase, experimentally determined; T_{gS}, the glass transition temperature of cross-linked pure soft segments, determined as explained below; and T_{gH}, is the glass transition of pure hard segments, its value, equal to 107°C in this case, was experimentally determined by Cuve et al.[1]

The T_{gS} could be determined as explained by Di Benedetto in Ref. 8. However, as noted by Pascault and Williams,[9] the easiest approach is constituted by the original equation of Di Benedetto quoted by Nielsen[10]:

$$\frac{T_{gS} - T_{g\infty}}{T_{g\infty}} = \frac{[(E_x/E_m) - (F_x/F_m)]X}{1 - (1 - F_x/F_m)X} \quad (5)$$

T_{gS} is the glass transition temperature of cross-linked polymer (soft segments); $T_{g\infty}$, the glass transition temperature of linear polymer, with infinite mass, obtained by extrapolation of T_g vs. $1/\overline{M_n}$ using different oligomers with different $\overline{M_n}$; X, the molar fraction of cross-linked constitutional units, assumed to be equal to $1/\overline{DP_n}$ here; E_x/E_m, the ratio of the lattice energies for cross-linked and uncross-linked polymer; and F_x/F_m, the ratio of the segmental mobilities for the same two polymers.

After Ref. 9,

$$F_x/F_m \approx 0 : E_x/E_m \approx 1.2$$

$$\frac{T_{gS} - T_{g\infty}}{T_{g\infty}} = \frac{1.2X}{1 - X} \quad (6)$$

For our PTMO product, $T_{g\infty}$ = −90°C = 183 K.

The knowledge of T_{gS} allowed the calculation of W_S and W_L in the soft phase and the volume fraction of the hard and soft phases. The results are shown in Table III.

In Table III, we can see that the T_g values of the soft phase are relatively low for $\overline{M_n} > 2000$; they are augmented for $\overline{M_n}$ = 1400 and 890. This augmentation is due to two effects: influence of the cross-linking by the hard blocks and the presence of the hard segments in the soft phase.

The microphase separation degree of soft segments exhibits an interesting variation: It is nearly constant with $\overline{M_n} > 2000$, attains a maximum value for $\overline{M_n}$ = 1410, and decreases when $\overline{M_n}$ = 890, the phase mixing being complete for PU 890 1/3/2, with low hard- and soft-segment lengths.

The maximum value for $\overline{M_n}$ = 1410 is singular. The explanation lays most probably in the particular morphology of this PU, which has, in this case, interconnected hard blocks. Seymour et al.[11] showed by infrared dichroism a change of the morphology of PU prepared with PTMO of $\overline{M_n}$ = 1000, MDI, and BD, when the percent of MDI varied from 24 to 28% (about 33% in weight of hard segments). This change of morphology is attributed to the formation of interconnected hard blocks. In our PU 1410 1/3/2, we very probably have the inversion of the phase with formation of a hard block interconnecting.

The hard phase of our PU contains crystalline parts whose proportion varies from 10 to 56%, with melting points found between 137 and 118 K. Any-

Table III Morphological Characteristics of PUR

Polyurethane	% in Weight of Soft Segments	% in Weight of Hard Segments	T_g of Soft Phase (°C)	Microphase Separation Degree of Soft Segments (%)	% in Weight				% in Volume[a]			
					Of Soft Segments	Of Hard Segments	Of Soft Segments	Of Hard Segments	Of Soft Segments	Of Hard Segments	Of Soft Segments	Of Hard Segments
					In Soft Phase		In Hard Phase		In Soft Phase		In Hard Phase	
PUR 2400 1/3/2	74.2	25.8	−75.0	63.6	47.2	4.2	27	21.6	50.2	3.4	28.7	17.7
					51.4		48.6		53.6		46.4	
PUR 2030 1/3/2	72.2	27.8	−76.2	61	44	2.7	28.2	25.1	47	2.2	30.1	20.6
					46.7		53.3		49.2		50.8	
PUR 2030 1/7/6	51.9	48.1	−80.8	63.4	32.9	0.4	19	47.7	37	0.3	21.4	41.3
					33.3		66.7		37.3		62.7	
PUR 1410 1/3/2	51.8	48.2	−70.3	73.6	38.1	3.3	13.7	44.9	42.9	2.9	15.4	38.9
					41.4		58.6		45.8		54.2	
PUR 890 1/3/2	41.7	58.3	−52.8	55.2	23	4.8	18.7	53.5	26.6	4.3	21.6	47.6
					27.8		72.2		30.9		69.1	
PUR 890 1/2/1	51.7	48.3	−47.8	No phase separation								

[a] Calculated from percentage in weight, with density of soft segments: 1.0; density of hard segments: 1.3.

Table IV Statistic Mechanical Characteristics of PUR

Polyurethane	% in Weight of Hard Segment	Young's Modulus E_0 (N/m^2)[a]	Stress at Break σ_R (N/m^2)[a]	Elongation at Break ε_R (%)[a]
PUR 2400 1/3/2	25.8	$5.9 \cdot 10^6$	$1 \cdot 10^7$	650
PUR 2030 1/7/6	48.1	$3.9 \cdot 10^7$	$1.6 \cdot 10^7$	530
PUR 1410 1/3/2	48.2	$5.5 \cdot 10^7$	$2.5 \cdot 10^7$	480
PUR 890 1/3/2	58.3	$1.7 \cdot 10^8$	$4.1 \cdot 10^7$	340
PUR 890 1/2/1	48.3	$1.6 \cdot 10^7$	$1.2 \cdot 10^7$	580

[a] Average of 3–5 measurements.

way, for the transport properties, the all-hard phase is considered as impermeable in comparison with the soft phase.

Static Mechanical Characterization

Table IV and the Figure 2 show the static mechanical characteristics of the studied PU. For PU at $\overline{M_n}$ constant ($\overline{M_n}$ = 2000 or $\overline{M_n}$ = 890), while E_0 and σ_r increases, ε_r decreases. The comparison between PU having the same percent of hard segments shows the differences of morphology with different $\overline{M_n}$ of soft segments. Therefore, for about 48% of hard segments and three values of $\overline{M_n}$ (2030, 1410, and 890), E_0 and σ_r have the highest values for PU $\overline{M_n}$ = 1410. The explanation should be the interconnection between hard segments in this PU 1410 1/3/2 forming the interconnected hard block as we have seen above, when for PU 2030 1/7/6, the microphase segregation degree being lower, there is a greater percentage of soft segments in the hard phase. For PUR 890 1/2/1, we have seen that there is complete mixing of hard and soft segments, giving the lowest values of E_0 and σ_r but the highest value of ε_R.

The static mechanical characterization shows once more the importance of morphology: The PU 1410 1/3/2, which corresponds to the phase inversion, has the best mechanical properties. What we have obtained is comparable to the results of Sung et al.[12,13] who studied the mechanical properties of two series of polyurethane–urea, prepared with PTMO of $\overline{M_n}$ = 1000 or 2000, toluene diisocyanate

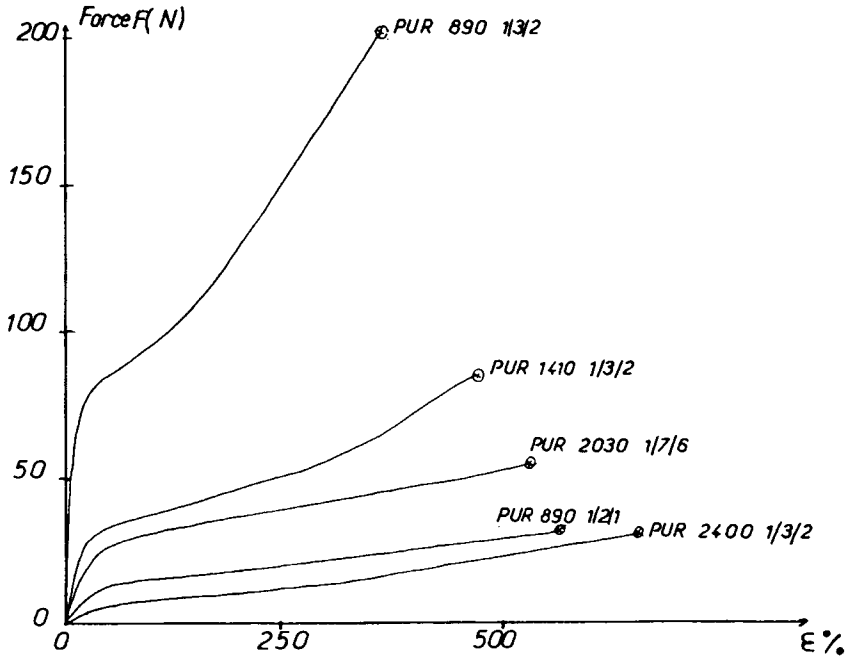

Figure 2 Static mechanical properties of studied PUR.

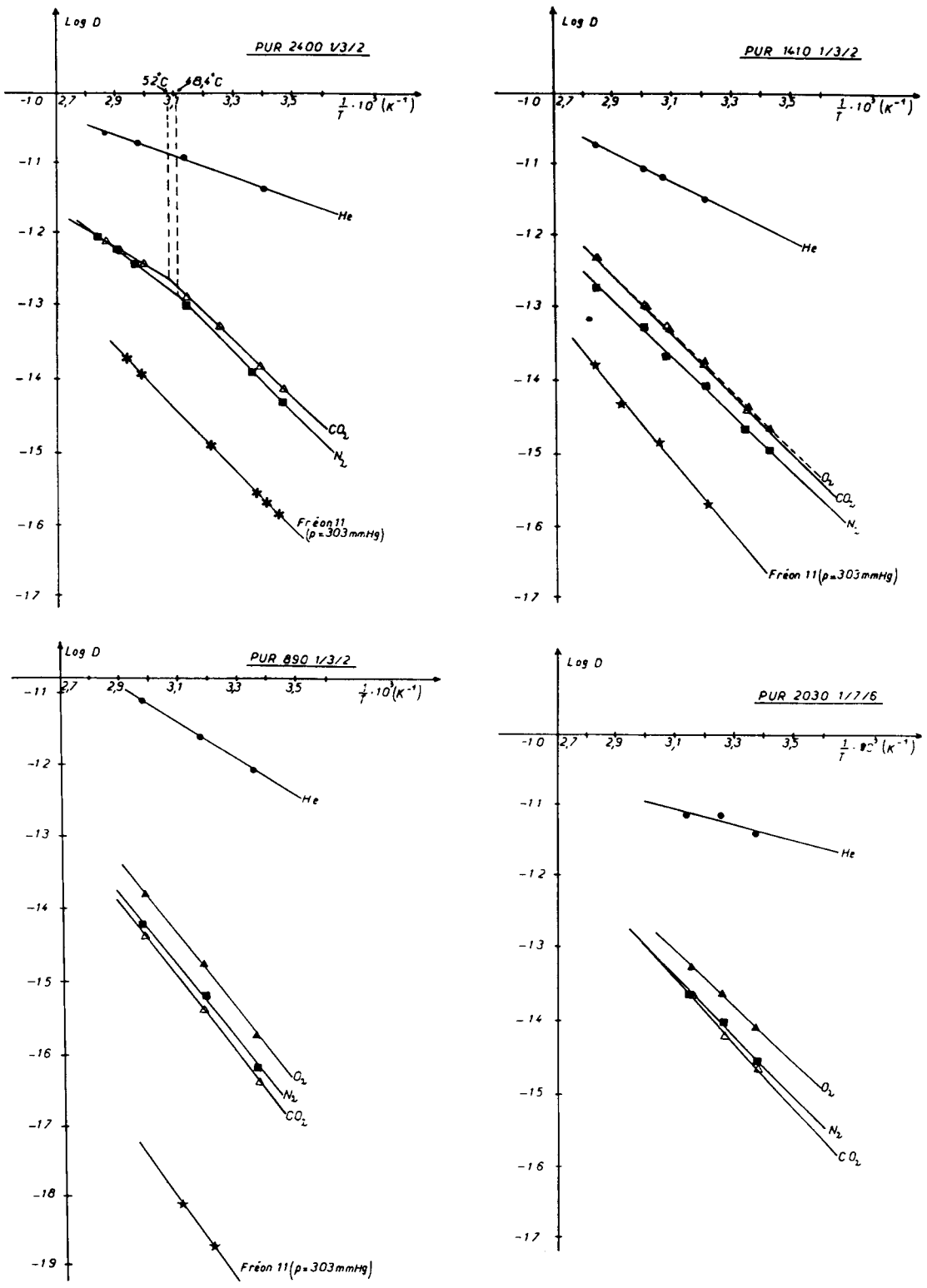

Figure 3 Log D vs. $1/T$ (D: diffusion coefficient).

(TDI), and ethylene diamine (ED), with the same percent of hard segments (30% in weight), with the formulation PTMO 1000/TDI/ED 1/2/1 giving a value of E_0 10 times higher than the one with the formulation PTMO 2000/TDI/ED 1/4/3. The σ_r values are, respectively, 400 and 200 kg/cm^2. The

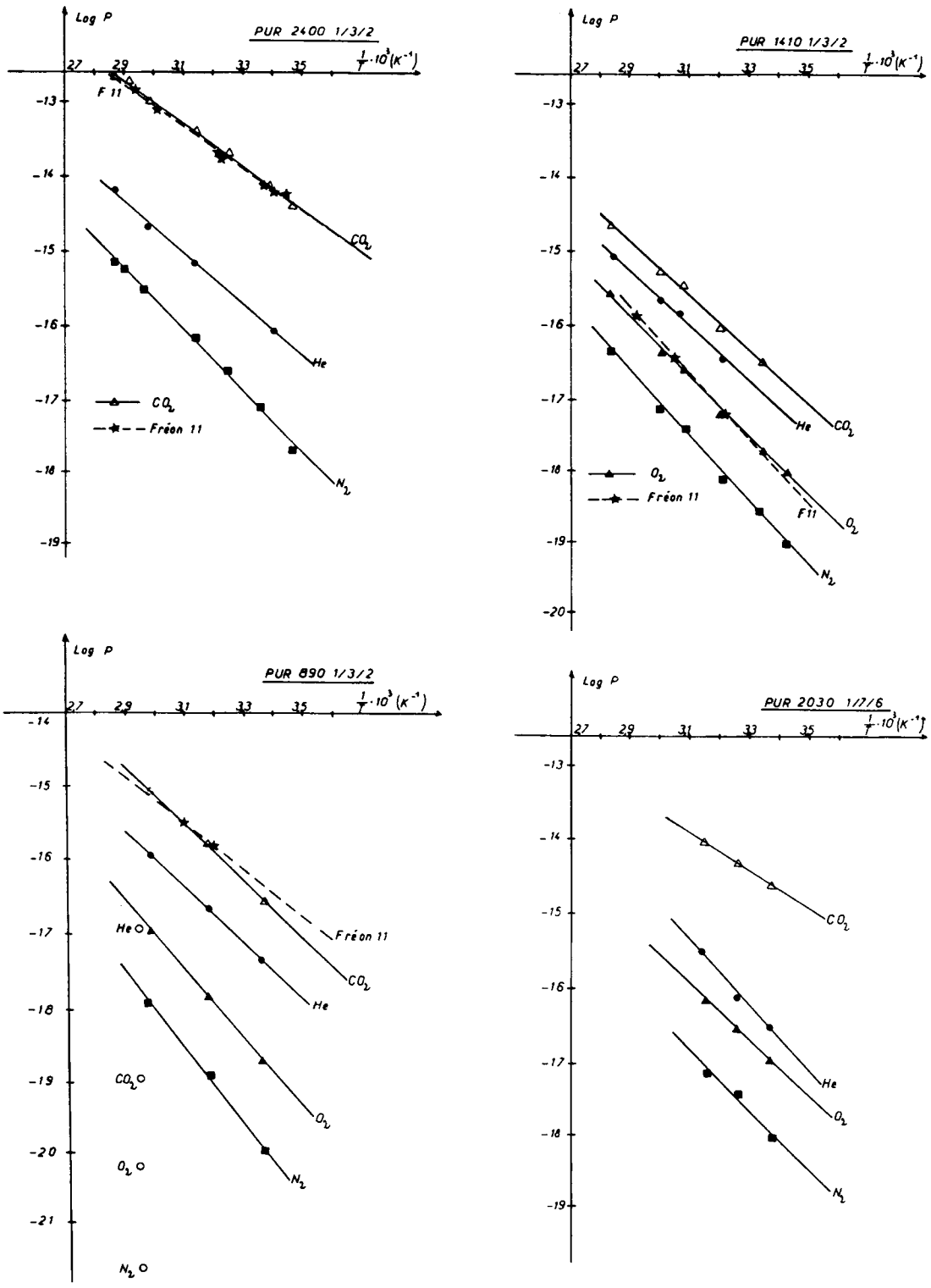

Figure 4 Log P vs. $1/T$ (P: permeability coefficient).

authors explained their results by the interconnection of hard block in the first product, whereas in the second, the hard segments are dispersed in a continuous soft phase.

Permeability Measurements

The Arrhenius graphs showing the neperian logarithm of diffusion, permeability, and solubility coef-

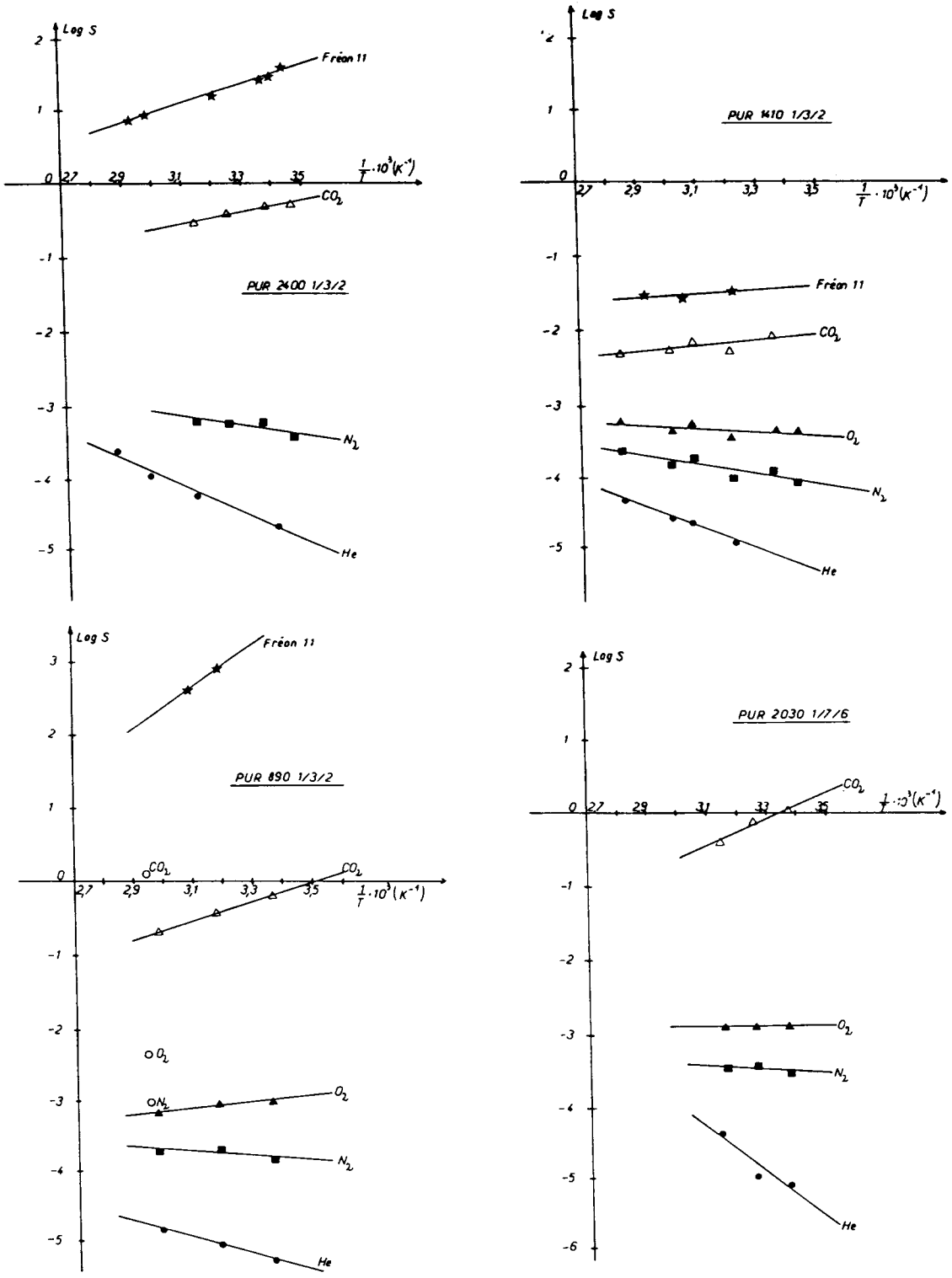

Figure 5 Log S vs. $1/T$ (S: solubility coefficient).

ficients vs. the inverse of absolute temperature are represented in Figures 3–5. The values of the preexponential terms D_0, P_0, and S_0 and activation energies E_D, E_P, and ΔH_S are given in Table V.

Table VI shows the values of diffusion, permeability, and solubility at 30°C for different gases and PUR. The comparison between our values and those given in the literature is difficult because the nature

Table V Diffusion, Permeability, and Solubility Arrhenius Parameters of Studied PUR

Polyurethane	Gases	D_0 (cm^2/s)	E_D (kcal/mol)	P_0 $\left\{\frac{cm^3\ (NTP)\ cm}{cm^2\ s\ atm}\right\}$	E_p (kcal/mol)	S_0 cm^3 (NTP cm^{-3} atm^{-1})	ΔH_S (kcal/mol)
PUR 2400	He	$1.77 \cdot 10^{-3}$	2.94	$1.23 \cdot 10^{-2}$	6.85	6.95	+3.91
1/3/2	N_2	$T < 48.4°C$ $T > 48.4°C$	$T < 48.4°C$ $T > 48.4°C$	$3.91 \cdot 10^{-2}$	8.27	$T < 48.4°C$ $T > 48.4°C$	$T < 48.4°C$ $T > 48.4°C$
		$6.16 \cdot 10^{-1}$ $3.77 \cdot 10^{-2}$	7.97 6.17			$6.35 \cdot 10^{-2}$ 1.04	+0.30 +2.10
	CO_2	$T < 52°C$ $T > 52°C$	$T < 52°C$ $T > 52°C$	$1.19 \cdot 10^{-2}$	5.72	$T < 52°C$ $T > 52°C$	$T < 52°C$ $T > 52°C$
		$3.88 \cdot 10^{-1}$ $5.20 \cdot 10^{-3}$	7.59 4.79			$3.07 \cdot 10^{-2}$ 2.29	−1.87 +0.93
	Freon 11	$2.07 \cdot 10^{-1}$	8.27	$8.60 \cdot 10^{-3}$	5.54	$4.16 \cdot 10^{-2}$	−2.73
PUR 1400	He	$7.15 \cdot 10^{-3}$	4.08	$1 \cdot 10^{-2}$	7.40	1.54	+3.32
1/3/2	N_2	$1.85 \cdot 10^{-1}$	7.75	$4.05 \cdot 10^{-2}$	9.23	$2.19 \cdot 10^{-1}$	+1.48
	O_2	$2.878 \cdot 10^{-1}$	7.82	$2.12 \cdot 10^{-2}$	8.28	$7.36 \cdot 10^{-2}$	+0.46
	CO_2	$4.23 \cdot 10^{-1}$	8.08	$1.42 \cdot 10^{-2}$	7.31	$3.36 \cdot 10^{-2}$	−0.77
	Freon 11	1.173	9.86	$8.55 \cdot 10^{-2}$	9.15	$7.29 \cdot 10^{-2}$	−0.71
PUR 1410	He	$2.96 \cdot 10^{-2}$	5.09	$7.76 \cdot 10^{-3}$	7.43	$2.62 \cdot 10^{-1}$	+2.34
1/3/2	N_2	1.98	10.01	$1.22 \cdot 10^{-1}$	10.61	$6.16 \cdot 10^{-2}$	+0.60
	O_2	4.10	10.20	$4.35 \cdot 10^{-2}$	9.27	$1.06 \cdot 10^{-2}$	−0.93
	CO_2	2.67	10.31	$2.79 \cdot 10^{-2}$	7.71	$1.04 \cdot 10^{-2}$	−2.60
	Freon 11	1.76	12.07	$2.76 \cdot 10^{-3}$	6.21	$1.56 \cdot 10^{-3}$	−5.87
PUR 2030	He	$5.22 \cdot 10^{-4}$	2.26	$1.53 \cdot 10^{-1}$	8.70	$2.93 \cdot 10^{-2}$	+6.45
1/7/6	N_2	$3.75 \cdot 10^{-1}$	8.03	$2.76 \cdot 10^{-2}$	8.54	$7.35 \cdot 10^{-2}$	+0.51
	O_2	$2.75 \cdot 10^{-1}$	7.59	$1.25 \cdot 10^{-2}$	7.47	$4.55 \cdot 10^{-2}$	−0.13
	CO_2	1.28	8.84	$2.28 \cdot 10^{-3}$	5.06	$1.78 \cdot 10^{-3}$	−3.79

Table VI Diffusion, Permeability, and Solubility Coefficients at 30°C of Studied PUR

Polyurethane	Gases	D at 30°C (cm^2/s)	P at 30°C $\left\{\frac{cm^3\ (NTP)\ cm}{cm^2\ s\ atm}\right\}$	S at 30°C $\{cm^3\ (NTP)\ cm^{-3}\ atm^{-1}\}$
PUR 2400	He	$1.38 \cdot 10^{-5}$	$1.51 \cdot 10^{-7}$	$1.09 \cdot 10^{-2}$
1/3/2	N_2	$1.20 \cdot 10^{-6}$	$4.63 \cdot 10^{-8}$	$3.86 \cdot 10^{-2}$
	CO_2	$1.41 \cdot 10^{-6}$	$9.45 \cdot 10^{-7}$	$6.70 \cdot 10^{-1}$
	Freon 11	$2.43 \cdot 10^{-7}$ [a]	$9.24 \cdot 10^{-7}$	3.80
PUR 1410	He	$8.54 \cdot 10^{-6}$	$5.43 \cdot 10^{-8}$	$6.36 \cdot 10^{-3}$
1/3/2	N_2	$5.14 \cdot 10^{-7}$	$9.83 \cdot 10^{-9}$	$1.91 \cdot 10^{-2}$
	O_2	$7.11 \cdot 10^{-7}$	$2.48 \cdot 10^{-8}$	$3.49 \cdot 10^{-2}$
	CO_2	$6.85 \cdot 10^{-7}$	$8.19 \cdot 10^{-8}$	$1.20 \cdot 10^{-1}$
	Freon 11	$1.00 \cdot 10^{-7}$*	$2.37 \cdot 10^{-8}$	$2.37 \cdot 10^{-1}$
PUR 890	He	$6.65 \cdot 10^{-6}$	$3.65 \cdot 10^{-8}$	$5.49 \cdot 10^{-3}$
1/3/2	N_2	$1.32 \cdot 10^{-7}$	$3.02 \cdot 10^{-9}$	$2.29 \cdot 10^{-2}$
	O_2	$2.01 \cdot 10^{-7}$	$9.95 \cdot 10^{-9}$	$4.95 \cdot 10^{-2}$
	CO_2	$1.10 \cdot 10^{-7}$	$8.38 \cdot 10^{-8}$	$7.62 \cdot 10^{-1}$
	Freon 11	$3.94 \cdot 10^{-9}$ [a]	$9.83 \cdot 10^{-8}$	$2.50 \cdot 10^{-1}$
PUR 2030	He	$1.26 \cdot 10^{-5}$	$8.86 \cdot 10^{-8}$	$7.04 \cdot 10^{-3}$
1/7/6	N_2	$6.65 \cdot 10^{-7}$	$2.11 \cdot 10^{-8}$	$3.16 \cdot 10^{-2}$
	O_2	$9.95 \cdot 10^{-7}$	$5.61 \cdot 10^{-8}$	$5.63 \cdot 10^{-2}$
	CO_2	$5.92 \cdot 10^{-7}$	$5.44 \cdot 10^{-7}$	$9.19 \cdot 10^{-1}$

[a] D values for Freon 11 are given at p = 303 Torr.

and percentage of components are different; but the values of permeability coefficients are about the same,[3,4] and our diffusion coefficient values are about 10 times higher than those given by Mac Bride et al.[2] The difference could due to the way PU was synthesized: in bulk for us and in solvent for Mac Bride et al.

For PU 2400 1/3/2, we can see a change of the slope of the graph Log $D = f(1/T)$ for two gases N_2 and CO_2. This phenomenon was also observed by Mac Bride et al.[2] and could be connected to the morphological transitions in this PU. This change of slope is not observed for the other PU, probably because the experiments were not effectuated in a sufficiently large range of temperature.

The permeation experiments with Freon 11 and PUR 2400 1/3/2 were effectuated at different pressures, p, of Freon. Figure 6 shows Log D vs. $1/T$ for different values of p (D is the value calculated from the classical formula $D = l^2/6\theta$). The variation of D vs. p (Fig. 7) is quasi-linear. For the permeability coefficient, it seems independent of p.

Only one value of pressure of Freon 11 is used for experiments with PU 1410 1/3/2 and PU 890 1/3/2. This value of 303 Torr corresponds to the vapor pressure of Freon 11 at 0°C; a more important pressure could break the PU membrane. These membranes are broken also when immerged in Freon 11, except the PU 1410 1/3/2, which has the morphology of the inversion region with interconnecting hard blocks.

In Figure 4, we can see the important permeability of CO_2 and Freon 11, which is more important than that of helium, and the relatively low values of their diffusion coefficients. We can affirm already the predominant role of their solubility and remark on the great exothermicity of their dissolution in PU. The diffusion and the solubility will be discussed separately.

Because of the multiphase morphology of PU, we made the hypothesis that the transport of gas is made essentially in the soft phase. The hard phase is considered as impermeable, and its presence is taken into account by a factor of tortuosity or factor of structure, K. Therefore, the diffusion coefficient, D, is equal to

$$D = D_S/K \tag{7}$$

where D_S represents the diffusion coefficient through the soft phase alone.

For filled polymers, different models permit the expression of the K value in respect to the volume fraction of the filler. Gulino[14] showed that all the

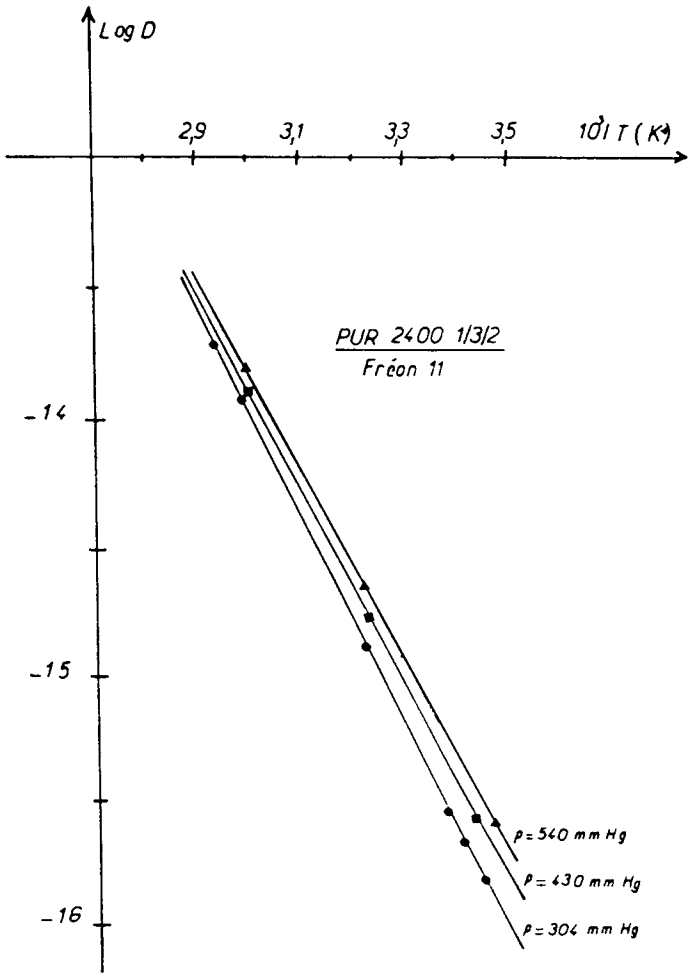

Figure 6 Log D vs. $1/T$ for Freon 11 through PUR 2400 1/3/2, at different vapor pressures.

theoretical models given in the literature are valuable as well except for the relatively high filler ratio and that the difference between two models is not important, even for two different sizes of filler particles.

For our PU cases, we used the simple relation of Maxwell[14]:

$$K = 1 + \frac{\phi_H}{2} \tag{8}$$

ϕ_H is the volume fraction of the hard phase, given in Table III. In fact, a change in K value does not provoke an appreciable variation of the diffusion coefficient. The error on ϕ_H derived from the one on W_H and ΔC_p could be estimated at about a few percent; so the relative error $\Delta D/D$ derived from $\Delta K/K$ should be lower to 1% and inferior to the contribution of the experimental error.

The behavior of the soft phase toward the diffusion is connected to the mobility of the soft segment, and, therefore, also to the length or the molecular weight $\overline{M_n}$. Andrady and Sefcik[5] found, in the case of reticulated PUs, a linear relation between Log P and $\overline{M_n}^{-1}$. As the solubility does not depend so much upon the reticulation density, the variation of P is due essentially to the variation of D. Hence, the next equation gives the expression of the diffusion coefficient, D, through the soft phase alone:

$$\begin{aligned} D &= D_S/[1 + \phi_H/2] \\ &= [D_0/(1 + \phi_H/2)]\exp(-1/\overline{M_n}) \end{aligned} \tag{9}$$

The experimental results, represented in Figure 8, seem to confirm this equation. It could be used for the determination of an approximated value of the diffusion coefficient of another PU.

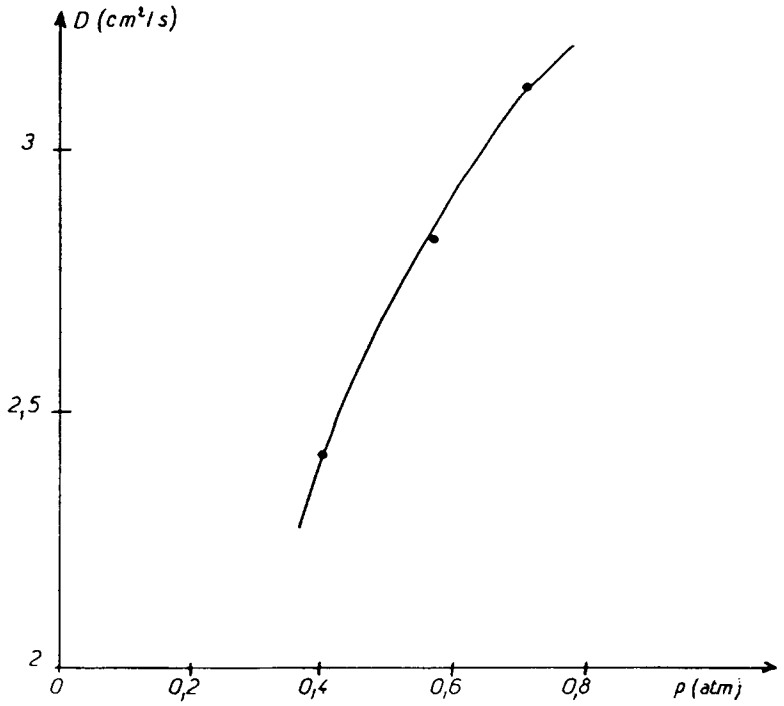

Figure 7 $D = f(P)$; D = diffusion coefficient at 30°C of Freon 11 through PUR 2400-1/3/2; P = pressure of F11.

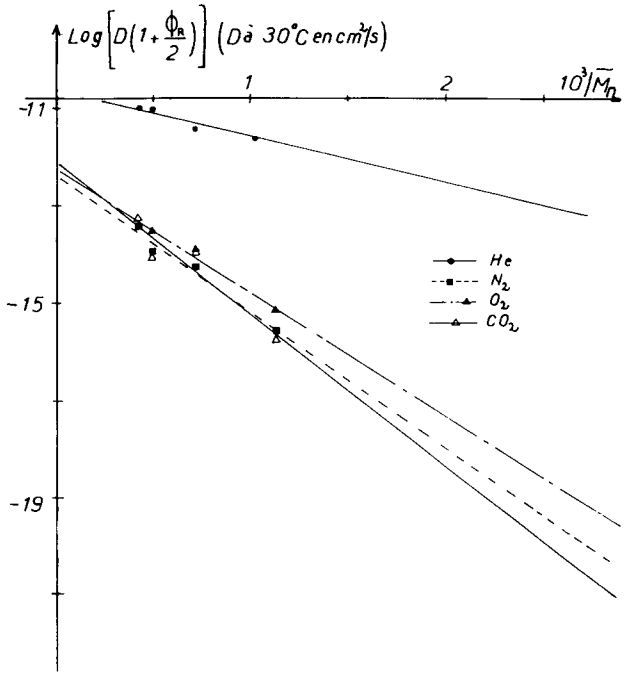

Figure 8 Log $\{D[1 + (\phi_H/2)]\} = f(1/\overline{M_n})$. D: diffusion coefficient experimentally determined; ϕ_H: volume fraction of hard phase, given in Table IV; $\overline{M_n}$: molecular mass of starting PTMO.

In the temperature range used in this study, the solubility coefficients of simple gas (He, N_2, O_2, and CO_2) obey the Arrhenius law:

$$S = S_0 \exp(-\Delta H_S/RT) \qquad (10)$$

where S_0 is the preexponential term, and ΔH_S, the dissolution energy. The S coefficients' values are less precise than the ones of D and P because S is calculated by P/D. It results in that S_0 and ΔH_S does not have precise values. But they are important because they give understanding about gas–polymer interactions.

Solubility and Morphology

The hypothesis presently formulated is the following: For the transport of a simple gas, the linear block PUs are equivalent to a polymer that contains some filler impermeable to the gas. Therefore, as in semicrystalline polymers where the solubility coefficient is proportional to the volume fraction of the amorphous phase, or in the case of filled polymer for which the solubility coefficient is proportional to the volume fraction of the nonfilled polymer, we

can write that the solubility coefficient of a simple gas in our PUs is proportional to the volume fraction ϕ_S of the soft phase:

$$S = S_S \phi_S \quad (11)$$

where S_S is the solubility coefficient in the soft phase alone.

For all the gases used in this study, the lowest values of S and S_S are obtained for the PUR 1410-1/3/2. It seems that the particular morphology of this PUR has influence on the solubility. Certainly, the hard phase is not totally impermeable to the gas and the morphology of a hard block interconnecting is the most efficient to diminish the solubility because the area of the interface between the hard phase and the soft phase is minimum.

Solubility and Physical Properties of Gas

From the preceding discussion, the values of S and S_S for different gases in a given PUR intervene at a constant factor or can be multiplied by a constant factor. Therefore, we can use these values although they are not exact.

From a thermodynamic point of view, most the authors[15-17] represent the dissolution process of the simple gas in the polymer as equivalent to the condensation of the gas followed by the mixing of the liquified gas in the polymer. Hence, we can predict that more important solubility coefficients are obtained if the gas is condensed more easily. Van Amerongen[16] and Barrer and Skirrow[18] found a linear relation between the logarithm of the solubility coefficient and the boiling points, T_b, or the critical temperatures, T_c, of the gas. A satisfactory thermodynamic treatment of this relation was given by Gee.[19]

Such a relation seems to exist between Log S_S and T_b and T_c for our PUs studied here except with Freon's values. Table VII collects the solubility coefficients at 30°C and the thermodynamic parameters of gas, and Figures 9 and 10 represent the neperian logarithm of the solubility coefficients of, respectively, T_b and T_c. In the case of Freon, the special behavior could be due to a strong interaction like hydrogen bound with PU.

The T_b and T_c values are the macroscopic parameters that measure the interaction between two molecules of gas. In the molecular scale, this inter-

Table VII Thermodynamical Parameters of Gases and Solubility Coefficients in PUR's Soft Phase at 30°C

Polyurethane	Volume Fraction of Soft Phase ϕ_s (%)	Gas	Boiling Temperature T_b (K)[a]	Critical Temperature T_c (K)[a]	Lenard-Jones Potential Constants ε/k (K)[b]	S at 30°C {cm^3 (NTP) cm^{-3} atm^{-1}}	S_S at 30°C {cm^3 (NTP) cm^{-3}}
PUR 2400		He	4.1	5.1	10	$1.09 \cdot 10^{-2}$	$2.03 \cdot 10^{-2}$
1/3/2	53.6	N_2	77.2	126.0	95	$3.86 \cdot 10^{-2}$	$7.20 \cdot 10^{-2}$
		CO_2	194.5 (subl.)	304.0	261	$6.70 \cdot 10^{-1}$	1.25
PUR 1410		He	4.1	5.1	10	$6.36 \cdot 10^{-3}$	$1.39 \cdot 10^{-2}$
1/3/2	45.8	N_2	77.2	126.0	95	$1.91 \cdot 10^{-2}$	$4.17 \cdot 10^{-2}$
		O_2	90.0	154.6	118	$3.49 \cdot 10^{-2}$	$7.62 \cdot 10^{-2}$
		CO_2	194.5 (subl.)	304.0	261	$1.20 \cdot 10^{-1}$	$2.62 \cdot 10^{-1}$
PUR 890		He	4.1	5.1	10	$5.49 \cdot 10^{-3}$	$1.78 \cdot 10^{-2}$
1/3/2	30.9	N_2	77.2	126.0	95	$2.29 \cdot 10^{-2}$	$7.41 \cdot 10^{-2}$
		O_2	90.0	154.6	118	$4.95 \cdot 10^{-2}$	$1.60 \cdot 10^{-1}$
		CO_2	194.5 (subl.)	304.0	261	$7.62 \cdot 10^{-1}$	2.47
PUR 2030		He	4.1	5.1	10	$7.04 \cdot 10^{-3}$	$1.89 \cdot 10^{-2}$
1/7/6	37.3	N_2	77.2	126.0	95	$3.16 \cdot 10^{-2}$	$8.47 \cdot 10^{-2}$
		O_2	90.0	154.6	118	$5.63 \cdot 10^{-2}$	$1.51 \cdot 10^{-1}$
		CO_2	194.5 (subl.)	304.0	261	$9.10 \cdot 10^{-2}$	2.46

[a] After Ref. 20.
[b] After Ref. 21.

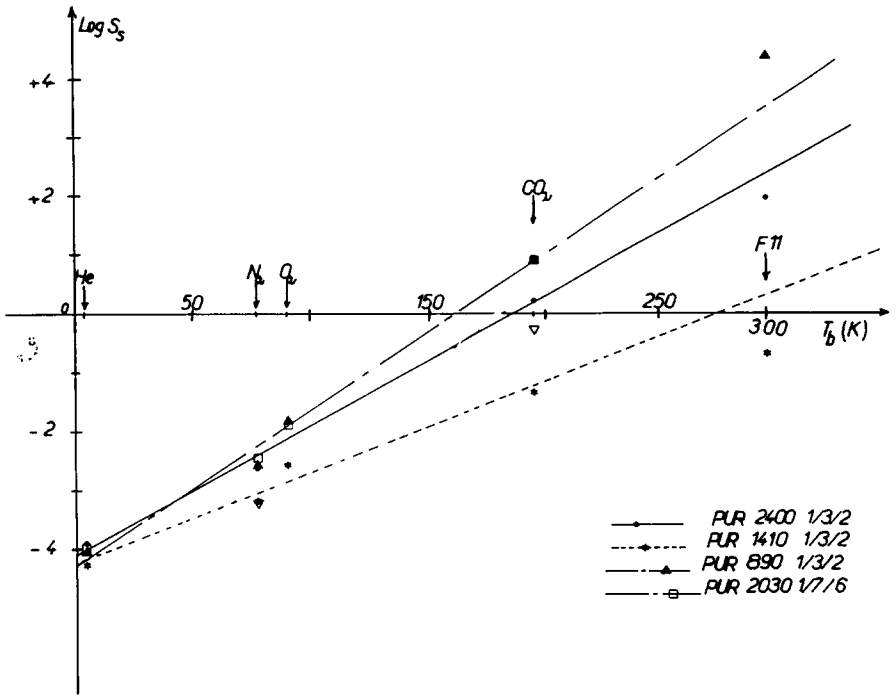

Figure 9 Log $S_S = f(T_b)$. S_S: solubility coefficient in soft phase; T_b: boiling temperature of gas.

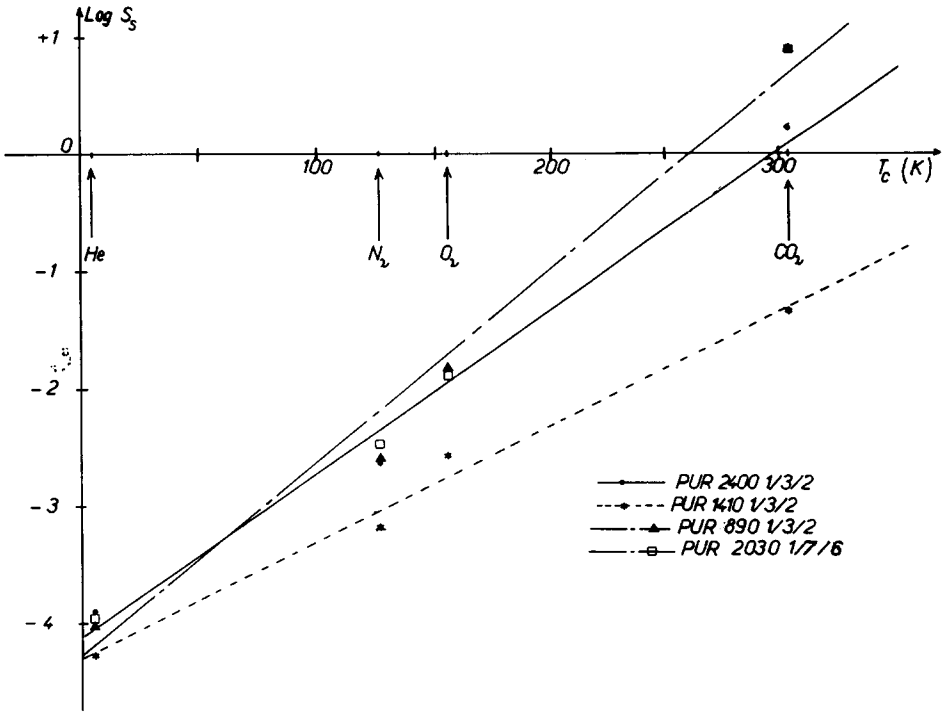

Figure 10 Log $S_S = f(T_c)$. S_S: solubility coefficient in soft phase; T_c: critical temperature of gas.

action can be measured by the ε/k constants of the Lennard-Jones potential of the gas. Michaels and Bixler[22] a linear relation between the neperian logarithm of the solubility coefficient S_a in the amorphous phase of polyethylene vs. the ε/k constants of gas. Jolley and Hildbrand[23] also experimentally established such a linear relation in the case of the solubility of the permanent gas in nonpolar solvents. Figure 11 shows that a linear relation also seems to exist between ε/k and Log S_S for our PUs.

Dissolution Energy and Lennard-Jones Potential

We have specified that numerous authors[15–17] represented the dissolution process of the simple gas in the polymer as thermodynamically equivalent to the condensation of the gas followed by the mixing of the liquified gas in the polymer. Therefore, the dissolution energy ΔH_S is the sum of the condensation energy ΔH_c and the mixing energy ΔH_m:

$$\Delta H_S = \Delta H_c + \Delta H_m \qquad (12)$$

According to the same authors, the condensation energy ΔH_c is negligible for the permanent gas at room temperature and ΔH_S is practically equal to the mixing energy ΔH_m. ΔH_m could be determined by the Hildebrand–Scatchard equation that is used generally for the dissolution of the polymers in solvents:

$$\Delta H_m = V_1(\delta_1 - \delta_2)^2\phi_2^2 \qquad (13)$$

For our cases, V_1 is the molar volume of liquified gas; δ_1 and δ_2, the solubility parameters of the gas and the polymer, respectively; and ϕ_2, the volume fraction of polymer in the polymer–gas blend.

In fact, this equation is not appropriate for our case. We have tried to use it without success. One of the difficulties is the estimation of V_1 and δ_1 of the gas at room temperature in a hypothetical liquid state.

For connecting ΔH_S to the physical properties of both gas and polymer, we consider that the gas–polymer interaction induces a variation of energy that is equal to ΔH_S. The energy of one molecule of gas in equilibrium with other molecules of gas is represented by ε_1, the constant of Lennard-Jones potential. This molecule of gas will have interaction with N polymer segments for which the energy be-

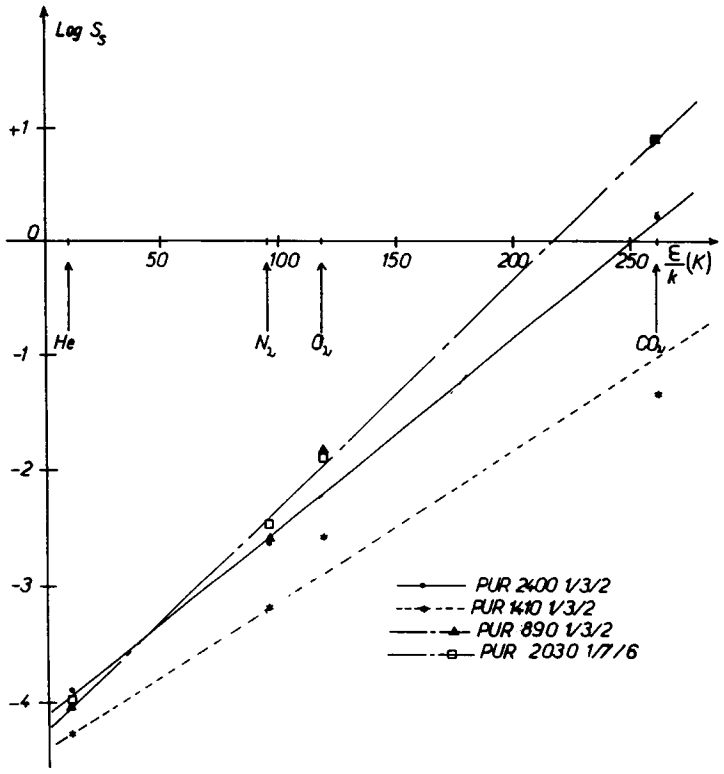

Figure 11 Log $S_S = f(\varepsilon/k)$. S_S: solubility coefficient in soft phase; ε/k: Lennard-Jones parameter of gas.

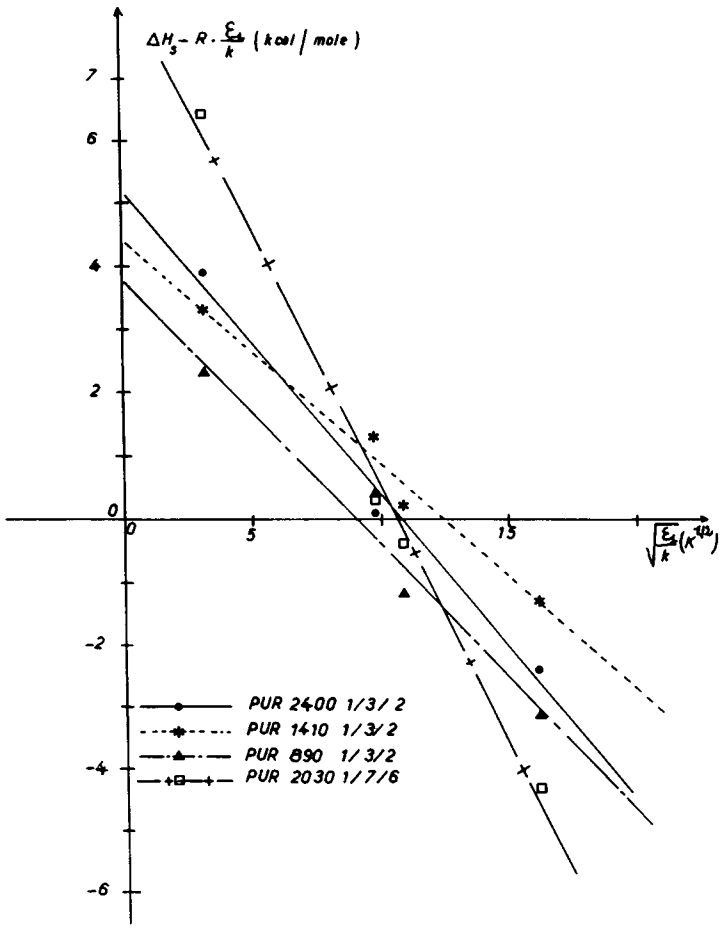

Figure 12 $[\Delta H_S - R \cdot \varepsilon_1/k] = f[(\varepsilon_1/k)^{1/2}]$. ΔH_S: dissolution energy; R: gas constant; ε_1/k: Lennard–Jones parameter of gas.

fore interaction is $f(N)\varepsilon_2$; $f(N)$ represents a function of N. If we applied the rule of geometrical average, the potential energy of the gas–polymer system has an expression like $f'(N)(\varepsilon_1\varepsilon_2)^{1/2}$.

The energy variation ΔE of the system is

$$\Delta E = \varepsilon_1 + f(N)\varepsilon_2 - f'(N)(\varepsilon_1\varepsilon_2)^{1/2} \quad (14)$$

For 1 mol of gas,

$$\Delta E(\text{kcal/mol}) = \frac{R}{k}[\varepsilon_1 + f(N)\varepsilon_2 - f'(N)(\varepsilon_1\varepsilon_2)^{1/2}] \quad (15)$$

R is the gas constant, and k, the Boltzmann constant. The Boltzmann law states that the population S of dissolved gas that is submitted to an energy variation ΔE is equal to

$$S = S_0 e^{-\Delta E/RT} \quad (16)$$

Therefore, ΔE is identical to ΔH_S, the dissolution energy. This approach, which is very qualitative, found experimental support in Figure 12, which represents $\Delta H_S - R \cdot \varepsilon_1/k$ in respect to $\sqrt{\varepsilon_1/k}$: The graphs are linear. We have also used with success the data of Michaels and Bixler[22] on the solubility of the gas in polyethylene for a similar representation.

CONCLUSION

For the segmented polyurethanes, the diffusion of gas seems be governed by the length of the soft segment; the free volume increases with this length and favors the diffusion. The solubility seems be greatly influenced by the morphology: The inversion-phase region with interconnected hard blocks is unfavorable to the solubility. The dissolution energy could be expressed in function of the constants of Lennard-Jones potential.

This work was sponsored by the Isover Saint-Gobain Co. The financial support of this institution is gratefully acknowledged. We wish to thank Mrs. M. Escoubes and MM Nguyen Quang Trong, Y. Camberlin, and J. P. Pascault for reading and discussing the manuscript.

REFERENCES

1. L. Cuvé, J. P. Pascault, and G. Boiteux, *Polymer,* **32,** 343 (1991).
2. J. S. Mac Bride, T. A. Massaro, and S. L. Cooper, *J. Appl. Polym. Sci.,* **23,** 201 (1979).
3. K. D. Ziegel, *J. Macromol. Sci.-Phys.,* **B5**(1), 11 (1971).
4. P. M. Knight and D. J. Lyman, *J. Membr. Sci.,* **17,** 245 (1984).
5. A. L. Andrady and M. D. Sefcik, *J. Polym. Sci. Polym. Phys. Ed.,* **22,** 237 (1984).
6. Y. Camberlin, J. P. Pascault, and Q. T. Pham, *Makromol. Chem.,* **397,** 180 (1979).
7. Y. Camberlin and J. P. Pascault, *J. Polym. Sci. Polym. Chem. Ed.,* **21,** 415 (1983).
8. A. T. Di Benedetto, *J. Polym. Sci. Polym. Phys. Ed.,* **25,** 1949 (1987).
9. J. P. Pascault and R. J. J. Williams, *J. Polym. Sci. Polym. Phys. Ed.,* **28,** 85 (1990).
10. L. E. Nielsen, *J. Macromol. Sci. Rev. Macromol. Chem.* **63,** 69 (1969).
11. R. W. Seymour, A. E. Allegrezza, and S. L. Cooper, *Macromolecules,* **6,** 896 (1973).
12. C. S. P. Sung, T. W. Smith, and N. H. Sung, *Macromolecules,* **13,** 117 (1980).
13. C. S. P. Sung, T. W. Smith, C. B. Hu, and N. H. Sung, *Macromolecules,* **12,** 538 (1979).
14. J. Gulino, Thesis Doctorat ès-Sciences, Lyon, 1981.
15. H. Yasuda, H. G. Clark, and V. Stannett, in *Encyclopedia of Polymer Science and Technology,* Wiley, New York, 1968, Vol. 9, 7, p. 794.
16. G. J. Van Amerongen, *J. Polym. Sci.,* **5,** 307 (1950).
17. D. Machin and C. E. Rogers, in *Encyclopedia of Polymer Science and Technology,* Interscience, New York, 1970, Vol. 12, p. 679.
18. R. M. Barrer and G. Skirrow, *J. Polym. Sci.,* **3,** 564 (1948).
19. G. Gee, *Q. Rev.,* **1,** 265 (1947).
20. *Handbook of Chemistry and Physics,* C. D. Hodgman (ed.). 63d ed. CRC Press, Boca Raton, FL, 1982–83.
21. American Institute of Physics Handbook, D. E. Gray (ed.). 3rd ed., McGraw-Hill, New York, 1972.
22. A. S. Michaels and H. J. Bixler, *J. Polym. Sci.,* **50,** 393 (1961).
23. J. E. Jolley and J. H. Hildebrand, *J. Am. Chem. Soc.,* **80,** 1050 (1958).

Received November 30, 1992
Accepted March 18, 1993